ZnO quantum dots synthesized by a vapor phase transport process

AUTHOR(S):

Lu, JG; Ye, ZZ; Huang, JY; Zhu, LP; Zhao, BH; Wang, ZL; Fujita, S

CITATION:

Lu, JG ...[et al]. ZnO quantum dots synthesized by a vapor phase transport process. APPLIED PHYSICS LETTERS 2006, 88(6): 063110.

ISSUE DATE:

2006-02-06

APPLIED PHYSICS LETTERS **88**, 063110 (2006)

ZnO quantum dots synthesized by a vapor phase transport process

J. G. Lu, Z. Z. Ye,[a] J. Y. Huang, L. P. Zhu, and B. H. Zhao
State Key Laboratory of Silicon Materials, Zhejiang University, Hangzhou 310027, People's Republic of China

Z. L. Wang
School of Materials Science and Engineering, Georgia Institute of Technology, Atlanta, Georgia 30332-0245

Sz. Fujita
International Innovation Center, Kyoto University, Katsura, Nishikyo-ku, Kyoto 615-8510, Japan

(Received 17 November 2005; accepted 11 January 2006; published online 8 February 2006)

A vapor phase transport growth process has been developed to synthesize ZnO quantum dots (QDs) on Si substrates. The characteristics were investigated for as-prepared ZnO QDs without any additional treatment. The formation of ZnO QDs with 6 nm in height and 15 nm in diameter is confirmed by scanning electron microscope and atomic force microscopy. Room-temperature photoluminescence reveals that the as-prepared ZnO QDs exhibit a predominant ultraviolet emission at 3.32 eV while the low energy defect-related blue-green emission is significantly quenched. The band gap of ZnO QDs is determined to be 3.41 eV, which evidently indicates the quantum confinement effects. © *2006 American Institute of Physics*. [DOI: 10.1063/1.2172154]

ZnO is a promising photonic material for use in the blue-UV region due to its direct band gap of 3.37 eV at room temperature with a large exciton binding energy of 60 meV, which are advantages for excitonic-related device applications.[1] The recent success of development of *p*-type ZnO makes these potentials more feasible.[2] In low-dimensional ZnO nanostructures, many significant exciton effects may be expected due to quantum confinement effects, and so the improvement in device performance can be predicted.[3] Among versatile ZnO nanostructures, quantum dots (QDs) are of great interest due to their fundamental importance as a three-dimensional confined system in bridging the gap between bulk matter and molecular species.

In the past two decades, ZnO QDs have been grown mainly using wet chemical methods.[4–8] The work on ZnO QDs grown on conventional solid substrates is quite scanty up to now. A study on ZnO QDs grown on solid substrates is important not only to understand the quantum confinement effects but also to create new forms of this material. Recently, a metalorganic chemical vapor deposition technique has been employed to produce ZnO QDs on SiO_2/Si substrates.[9,10] However, regardless of the preparation methods, the UV luminescence in as-prepared ZnO QDs is strongly quenched while the low energy defect-induced visible emission commonly dominates the photoluminescence (PL) spectrum unless additionally elaborated treatments (e.g., surface modification,[4–7] or postdeposition annealing[8–10]) are performed. In these regards, the realization of predominant UV luminescence in as-prepared ZnO QDs is strongly demanded in order to realize nanoscale multifunctional devices. Our motivation is to provide a feasible method to realize the predominant UV luminescence in as-prepared ZnO QDs on solid substrates without any additional treatment. A vapor phase transport (VPT) deposition process, having been extremely successful in creating ZnO nanomaterials, such as nanowires and nanorods,[11] was proposed in this work to produce ZnO QDs on Si substrates. A strong and predominant UV luminescence has been realized in the as-prepared ZnO QDs.

Our fabrication of ZnO QDs was conducted in a horizontal tube furnace. The system is shown in Fig. 1. Zinc acetate dihydrate was used as the basic source materials after being dried at 102 °C for 2 h to remove the water of crystallization. Si (111) wafers were used as the substrates. The furnace temperature was set as at 500 °C in the growth process. There was a flat-temperature zone (500 °C) at the center location of the furnace, and the temperature gradient at the location between the center and the end of the furnace was approximately 300 °C. The substrate was placed downstream of a 20% O_2/Ar mixture gas flow in the 440–460 °C zone prior to growth. The source materials, placed at the closed end of a slender one-end-sealed quartz tube, were drawn into the furnace when its temperature was ramped to 500 °C and positioned at the center of the furnace. The furnace temperature (500 °C) was typically kept 3 min under a constant O_2/Ar flow of 10 sccm in atmospheric pressure, and then the source materials were drawn out from the furnace. The samples collected on the substrates were furnace cooled down to room temperature.

The morphologies of the products were investigated by a FEI Sirion 200 FEG field-emission scanning electron microscope (SEM) and a ZAFM-II atomic force microscopy

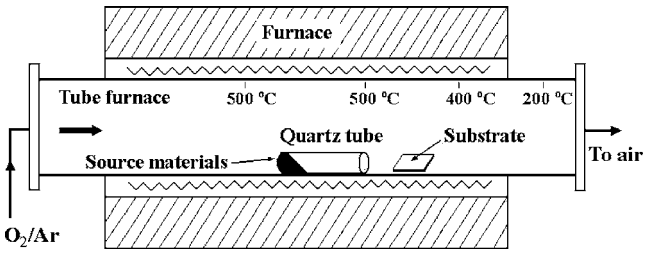

FIG. 1. Schematic diagram of experimental apparatus for growth of ZnO QDs.

[a]Electronic mail: yezz@zju.edu.cn

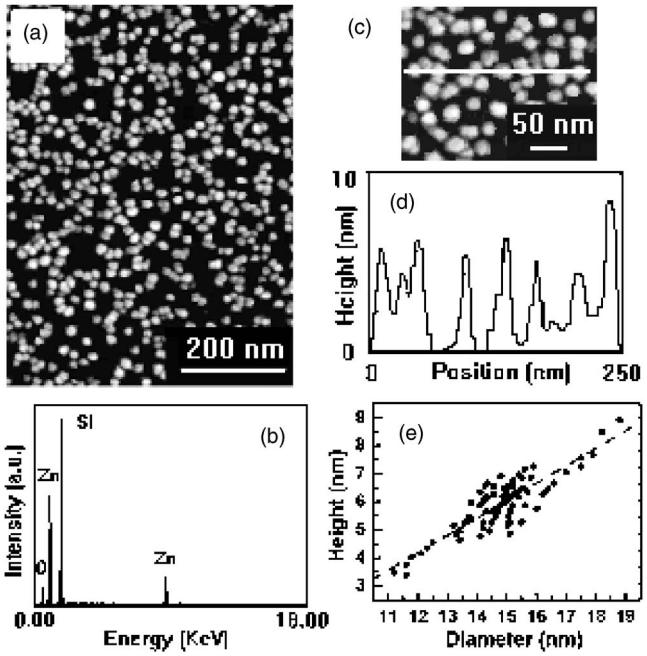

FIG. 2. (a) Surface SEM image of the as-prepared ZnO QDs. (b) EDX spectrum corresponding to the area of Fig. 2(a) showing the chemical composition of nanodots. (c) Plan-view AFM image of the as-prepared ZnO QDs. (d) Linearly scanned profile of the surface morphology along the solid line marked in Fig. 2(c). (e) Dot dimension distribution of individual QDs determined by AFM measurements. The dashed line in Fig. 2(e) is the slope obtained by the linear fitting of all the points.

(AFM) in a contact mode. The chemical composition was analyzed by using an energy dispersive x-ray (EDX) spectroscopy attached to the SEM. X-ray diffraction (XRD) analysis was carried out on a Bede D1 system with Cu $K\alpha$ radiation ($\lambda = 0.1541$ nm). Photoluminescence (PL) measurements were performed at room temperature by using a He–Cd laser (325 nm) as the excitation source. Absorption was measured with a Lambda 20 UV-visible spectrometer.

Figures 2(a) and 2(c) illustrate the SEM and AFM images, respectively. The images clearly identify the formation of ZnO QDs. The nanodot density is 2×10^{11} cm^{-2} and the average diameter is 15 nm. They are of a narrow size distribution, and essentially no obvious aggregation can be found. But, the nanodots are not spherical in shape. The average height given by the AFM image [Figs. 2(d) and 2(e)] is about 6 nm. The EDX pattern of ZnO QDs is shown in Fig. 2(b). The chemical composition of the nanodots is Zn and O as expected (Si comes from substrate), and no other elements (e.g., C) are present. The atomic percents (at. %) of Zn and O in the matrix are 50.2% and 49.8%, respectively. Figure 3(a) is the XRD profile of ZnO QDs. The diffraction peaks and interplane spacings are well matched to the standard diffraction pattern of wurtzite ZnO [Fig. 3(b)], demonstrating the formation of wurtzite ZnO nanocrystals. These results indicate that the obtained ZnO QDs are of acceptable quality with high chemical purity and stoichiometric composition.

Zinc acetate is prone to decomposition above its melting point of 235 °C. In the growth process, zinc acetate was heated rapidly to 500 °C, so the decomposition occurred intensively, resulting in a relatively oxygen-deficient condition in quartz tube

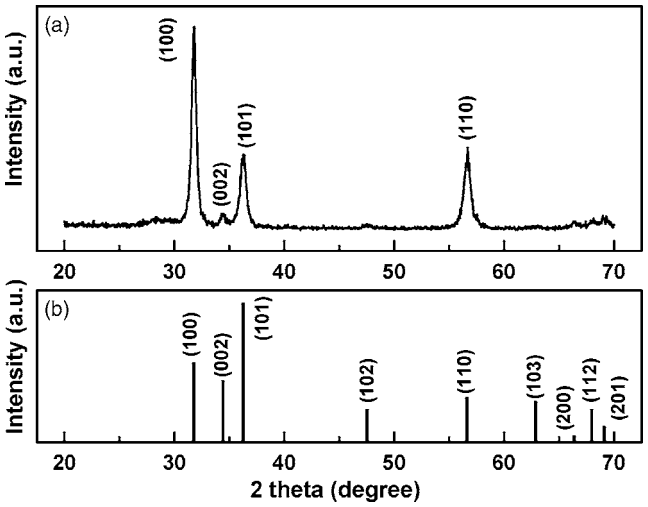

FIG. 3. (a) X-ray diffraction pattern of ZnO QDs. (b) Diffraction peaks of the bulk wurtzite ZnO.

$$\mathrm{Zn(CH_3COO)_2}(s) \rightarrow \mathrm{Zn}(v) + 2\mathrm{CH_3COO}(s^*), \quad (1)$$

where s, v, and s^* represent solid, vapor, and activated states, respectively. Zn vapor subsequently flows out of the tube and condenses on the substrate forming liquid droplets, which are ideal nuclei of crystals. This nucleation acts as a sink for migrating surface adatoms and consumes adsorbed species transported by surface diffusion, which responds to the formation of ZnO QDs in an O_2/Ar ambient

$$\mathrm{Zn}(\ell) + \mathrm{O_2}(g) \rightarrow \mathrm{ZnO}(s), \quad (2)$$

where ℓ and g represent liquid and gas, respectively. This is a typical vapor phase transport (VPT) growth process. In a conventional VPT process a mixture of ZnO and graphite powders was commonly used as the basic source materials and the process was performed typically above 1000 °C.[3,11] At this high temperature one can hardly use a Si wafer as a substrate, and it is necessary to use an Al_2O_3 wafer, even though Si substrates have advantages in terms of easy transformation into electronic devices and low price. In this work we use zinc acetate as the basic source material and so the growth temperature can be lower than 500 °C. At this low temperature one can conveniently use Si wafers as substrates to produce ZnO nanomaterials.

Figure 4 shows the global room-temperature PL spectrum of the as-grown ZnO QDs. The UV emission (3.32 eV) is strong and predominant in the PL spectra, while the low energy blue-green band (around 2.57 eV), which is mainly attributed to surface defect levels associated with oxygen vacancies or zinc interstitials,[7,10] is significantly quenched. It is an exciting result. There are few reported so far in realizing prominent UV emission in as-prepared ZnO QDs. The accessional treatments such as surface modification and postdeposition annealing are commonly needed to obtain a prominent UV emission in ZnO QDs.[4–10] These demonstrate a low defect density and high optical quality for the ZnO QDs obtained here. In addition, it should be noted that the UV PL peak (3.32 eV) is located at a high energy with reference to the near-band-edge (NBE) emission near 3.26 eV commonly seen at room temperature in ZnO bulk crystals or thin films.[12] The 3.32 eV peak has never been observed in the room-temperature PL spectra of ZnO bulk crystals or thin

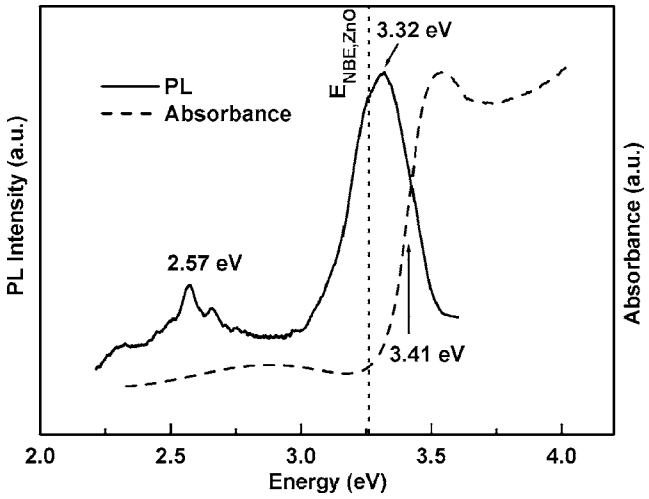

FIG. 4. Optical adsorption and PL spectra of ZnO QDs measured at room temperature. Dotted line is the NBE emission line commonly seen in ZnO bulk crystals or thin films.

films. Thus, the UV emission of ZnO QDs is ascribed to the quantum-confined band-edge emission due to the quantum size effects.[13]

In Fig. 4 the optical adsorption spectrum of the as-grown ZnO QDs is also shown. These nanodots exhibit strong free exciton adsorption at room temperature with quantum size effects. Here, we use the derivative of the adsorption curve developed in Ref. 14 to determine the band gap of ZnO QDs. The value is determined to be 3.41 eV, which is significantly larger than that (3.37 eV) of bulk ZnO and shows the quantum confinement effects. The band gap (E) of ZnO QDs can also be theoretically calculated from the nanodot sizes based on the effective mass approximation.[15] The average height and average diameter of nanodots are 6 and 15 nm, respectively, as mentioned above. It should be noted that the dot diameter is always overestimated due to the distortion of AFM and SEM images, but fortunately the height is not affected by the distortion introduced and so it is precise.[16] Since the dimension of nanodots is much larger than the excitonic Bohr radius of 1.8 nm for ZnO, they will experience a weak confinement circumstance[15]

$$E = E_g + \frac{\hbar^2\pi^2}{2}\left(\frac{1}{m_e^*} + \frac{1}{m_h^*}\right)\left(\frac{1}{h^2} + \frac{2}{d^2}\right) - E_{\mathrm{ex}},$$

where E_g, E_{ex}, and $\hbar$ are the bulk band gap (3.37 eV), the bulk exciton binding energy (60 meV), and Planck's constant, respectively. Also, h and d are the nanodot height and diameter, respectively. The electron and hole effective masses are $m_e^*=0.24\ m_0$ and $m_h^*=0.45\ m_0$, respectively, for ZnO. It is worth noting that the band gap (E) of ZnO QDs is mainly determined by the height of nanodots. The calculated band gap is 3.42 eV, which agrees well with the experimental data.

There is a ~90 meV blueshift of adsorption edge from the emission line, referred to as the Stokes shift. The Stokes shift, having the ability to quantify the degree of excitonic localization, is widely used as a negative indicator of sample quality. The Stokes shift of 90 meV is very low as compared with that reported (>300 meV) in ZnO QDs synthesized by the wet chemical method,[7] which suggests the high quality of ZnO QDs obtained by the VPT process provided here.

In summary, we have provided a VPT growth process to produce ZnO QDs with quantum confinement effects on Si substrates. The dimension of nanodots is 6 nm in height and 15 nm in diameter. ZnO QDs are of high chemical purity and stoichiometric composition with wurtzite structure. A strong and predominant UV emission can be achieved in as-prepared ZnO QDs at room temperature, and no additional treatment is needed. The quantum confinement effects from ZnO QDs are well confirmed by the optical adsorption and PL spectra.

This work was supported by the National Natural Science Foundation of China under Contract No. 90201038.

[1]Z. K. Tang, G. K. L. Wong, P. Yu, M. Kawasaki, A. Ohtomo, H. Koinuma, and Y. Segawa, Appl. Phys. Lett. **72**, 3270 (1998).
[2]J. G. Lu, Z. Z. Ye, F. Zhuge, Y. J. Zeng, B. H. Zhao, and L. P. Zhu, Appl. Phys. Lett. **85**, 3134 (2004).
[3]Z. L. Wang, J. Phys.: Condens. Matter **16**, R829 (2004).
[4]E. M. Wong, J. E. Bonevich, and P. C. Searson, J. Phys. Chem. B **102**, 7770 (1998).
[5]C. M. Mo, Y. H. Li, Y. S. Liu, Y. Zhang, and L. D. Zhang, J. Appl. Phys. **83**, 4389 (1998).
[6]L. Guo, S. Yang, C. Yang, P. Yu, J. Wang, W. Ge, and G. K. L. Wong, Appl. Phys. Lett. **76**, 2901 (2000).
[7]C. L. Yang, J. N. Wang, W. K. Ge, L. Guo, S. H. Yang, and D. Z. Shen, J. Appl. Phys. **90**, 4489 (2001).
[8]H. Zhou, H. Alves, D. M. Hofmann, W. Kriegseis, B. K. Meyer, G. Kaczmarczyk, and A. Hoffmann, Appl. Phys. Lett. **80**, 210 (2002).
[9]S. W. Kim, Sz. Fujita, and Sg. Fujita, Appl. Phys. Lett. **81**, 5036 (2002).
[10]K. K. Kim, N. Koguchi, Y. W. Ok, T. Y. Seong, and S. J. Park, Appl. Phys. Lett. **84**, 3810 (2004).
[11]Y. N. Xia, P. D. Yang, Y. G. Sun, Y. Y. Wu, B. Mayers, B. Gates, Y. D. Yin, F. Kim, and H. Q. Yan, Adv. Mater. (Weinheim, Ger.) **15**, 353 (2003).
[12]L. Wang and N. C. Giles, J. Appl. Phys. **94**, 973 (2003).
[13]V. A. Fonoberov and A. A. Balandin, Appl. Phys. Lett. **85**, 5971 (2004).
[14]S. Srinivasan, F. Bertram, A. Bell, F. A. Ponce, S. Tanaka, H. Omiya, and Y. Nakagawa, Appl. Phys. Lett. **80**, 550 (2002).
[15]Y. Kayanuma, Phys. Rev. B **38**, 9797 (1988).
[16]R. M. Sassaki, R. A. Douglas, M. U. Kleinke, and O. Teschke, J. Vac. Sci. Technol. B **14**, 2423 (1996).